Search for $\tau \to 3\mu$ decays with CMS experiment at LHC

Federica M. Simone[1⋆] on behalf of the CMS Collaboration

1 Università di Bari & INFN Bari
⋆ federica.maria.simone@cern.ch

December 8, 2021

16th International Workshop on Tau Lepton Physics (TAU2021),
September 27 – October 1, 2021
doi:10.21468/SciPostPhysProc.?

Abstract

New results are presented for a search for charged lepton flavor violating decays of tau leptons to three muons with the CMS detector. The search employs tau leptons produced in decays of heavy flavor B or D mesons and W bosons.

1 Introduction

The extension of the Standard Model (SM) to include mass eigenstates for the neutrinos allows for lepton flavor violation (LFV) also involving charged leptons. Nevertheless, LFV decays such as $\tau \to 3\mu$ are predicted with strongly suppressed branching fractions in the context of the extended SM [1]. Any observation of such a decay would indicate the presence of new physics. On the other hand, many Beyond the Standard Model (BSM) theories predict LFV decays with sizeable branching fractions accessible by present day experiments [2, 3].

The $\tau \to 3\mu$ decay is a promising channel for searching for LFV at hadron colliders given the large quantity of tau leptons that can be produced and the clean experimental signature provided by the three final-state muons.

The search for this decay has already been carried out by several experiments and no evidence has been observed so far. Table 1 summarises the upper limits on the $\tau \to 3\mu$ branching fraction set by different HEP experiments both at e^+e^- and pp colliders. The stricter limit on the branching fraction has been set by the Belle collaboration with $\mathcal{B}(\tau \to 3\mu) < 2.1 \cdot 10^{-8}$ at 90% confidence level [4].

In this contribution we present the search for $\tau \to 3\mu$ decays at the CMS experiment [5] in proton-proton collisions at $\sqrt{s} = 13$ TeV centre-of-mass energy [6]. The analysis is performed on data recorded by CMS in 2016, accounting for an integrated luminosity of 33.2 fb^{-1}. The analysis targets τ leptons produced in c- and b-flavored mesons (mostly D_s, B^0, $B^\pm$) also referred to as *heavy flavor*, and taus produced in W vector boson decays. Inclusion of charge-conjugate states is implied throughout this paper.

2 Analysis in the heavy flavor channel

The dominant sources of τ leptons at the LHC are hadrons containing c or b quarks (primarily D and B mesons with a small contribution from c/b-baryons), the largest fraction of taus being produced in $D_s \to \tau(3\mu)\nu$, $B^0 \to \tau(3\mu)$X and $B^+ \to \tau(3\mu)$X decays, accounting for $\sim 94\%$ of the total τ lepton production.

Table 1: Summary of the upper limits on the $\tau \to 3\mu$ branching fraction set by different HEP experiments both at e^+e^- and pp colliders.

Pub. year	Experiment	Source of τ leptons	Exp. [*]	Obs. [*]
2010 [4]	Belle	$e^+e^- \to \tau\tau$	-	2.1
2010 [7]	BaBar	$e^+e^- \to \tau\tau$	4.0	3.3
2014 [8]	LHCb	$D/B \to \tau X$ (Run 1)	5.0	4.6
2016 [9]	ATLAS	$W \to \tau\nu$ (Run 1)	39	38

$[*] \times 10^{-8}$ at 90% C.L.

The measurement of the $\tau \to 3\mu$ branching fraction for τ leptons produced in the heavy flavor channel can be performed with reduced uncertainties by using the $D_s \to \phi(\mu\mu)\pi$ decays as a normalisation channel.

Simulated Monte Carlo (MC) samples are used to model the signal and estimate the production of τ leptons, where the $\tau \to 3\mu$ is assumed to be a model-independent 3-body phase-space decay, while the simulation of the $D_s \to \phi(\mu\mu)\pi$ decay allows for validating the MC samples.

The analysis strategy for the $\tau \to 3\mu$ search in the heavy flavor channel is developed targeting three muons forming a good common vertex in the kinematic phase space of the signal, the 3μ vertex (secondary vertex or SV) being displaced with respect to the primary vertex (PV) from pp collision. In the presence of signal, the invariant mass of the three muons is expected to form a narrow peak at the τ lepton mass over a smoothly distributed background.

2.1 Event selection and categorisation

Events are collected by mean of a high-level trigger (HLT) requiring two muons with $p_T > 3$ GeV and one charged track with $p_T > 1.2$ GeV, with common vertex significantly displaced with respect to the beamline. The invariant mass of the 3μ system is required to be within 1.60–2.02 GeV. The HLT is also compatible with $D_s \to \phi(\mu\mu)\pi$ events.

Collected events are selected offline by requiring the total charge of the 3μ to be ± 1, and events with opposite-charged muon pairs with 2μ invariant mass compatible with the $\omega(783)$ or the $\phi(1020)$ resonances are discarded.

Data events are split based on the $m(3\mu)$ invariant mass into a signal region ($[1.75, 1.80]$ GeV) and a sideband region ($[1.60, 1.75] U [1.80, 2.00]$ GeV). Events in the mass sidebands are used to describe the background. The trajectory of the selected $\tau \to 3\mu$ candidate is extrapolated to the beamline and the PV is selected as the vertex closest to the extrapolated point.

In order to enhance the sensitivity of the search, events are categorised based on the relative resolution on the $m(3\mu)$ invariant mass (σ_m/m), shown in Figure 1. Events are split in three mass resolution bins: $\sigma_m/m < 0.7\%$, $\sigma_m/m \leq 0.7\%$ and $\sigma_m/m > 1.0\%$, $\sigma_m/m \leq 1.0\%$. There are three resulting categories are labeled A, B, and C, being characterised by an average $m(3\mu)$ resolution of 12, 19 and 25 MeV respectively. The pseudorapidity of the decay products correlates with the σ_m/m resolution, category C being mostly populated by τ produced in the endcaps of the detector.

2.2 Training of the Boosted Decision Tree

A boosted decision tree (BDT) is trained to reject background events in data. In the training, the signal sample is build by mixing $D_s \to \tau(3\mu)\nu$, $B^0 \to \tau(3\mu)$X and $B^+ \to \tau(3\mu)$X MC simulated events, while data events in the 3μ mass sidebands are used as background. A set

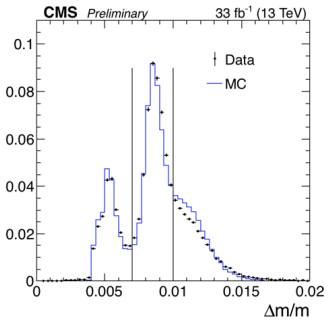

Figure 1: Distributions of $m(3\mu)$ invariant mass resolutions for simulated $\tau \to 3\mu$ events (solid line) and 3μ sideband data events (dots), passing all selection criteria. The vertical lines at $\sigma_m/m = 0.007$ and 0.01 separate three event categories (A, B, and C) used in the analysis [10].

of 10 observables is used in the training: the smallest muon momentum, three distinct muon quality criteria (each using the "worst" value of the three muon candidates), the χ^2 of the 3μ vertex fit, the angle between the 3μ momentum vector and the vector connecting the the SV and the PV (the *pointing angle*), the significance of the SV-PV distance, the smallest transverse impact parameter (IP) of the muons with respect to the PV, the smallest distance of closest approach to the SV of all other tracks in the event with $p_T > 1$ GeV, and the summed p_T of all tracks surrounding the muon divided by the p_T of the muon candidate. For the last two variables, the largest value among the three muons is used. Figure 2 shows the signal and background distributions for the three observables with the best discriminating power used for the BDT training.

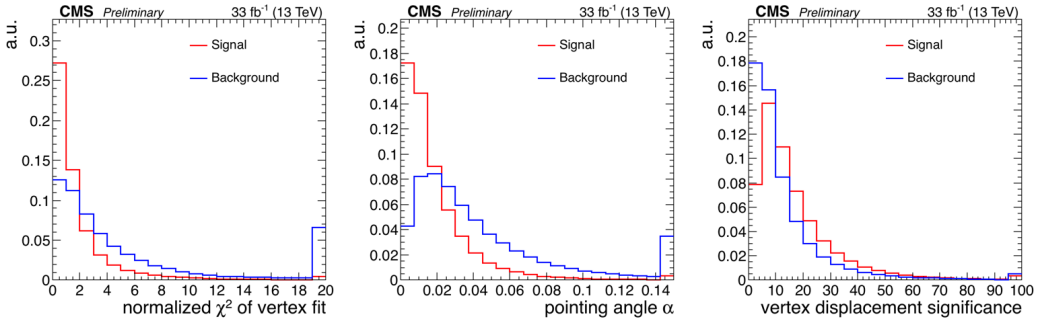

Figure 2: Signal and background distributions for the three observables with the best discriminating power used for the BDT training: (left) normalised χ^2 of the 3μ vertex fit; (center) the angle between the 3μ momentum vector and the vector connecting the primary and 3μ vertices; (right) significance of the 3μ vertex displacement. All distributions are normalised to unity [10].

Events are further categorised in three sub-categories based on the BDT score for the purpose of retaining the two sub-categories with best signal-to-background purities. The boundaries are set by maximising the expected search sensitivity and labelled 1, 2 and 3, where events in sub-category 3 are discarded. Thus, six independent event categories are formed: A1, A2; B1, B2; C1, C2. In these six categories, the $m(3\mu)$ mass is fitted with an exponential function and compared to the expected signal assuming $\mathcal{B}(\tau \to 3\mu) = 10^{-7}$, as shown in Figure 3. The signal is modelled with a Gaussian plus Crystal Ball function with fixed mean and width, as determined from fitting the simulated signal in each mass resolution category.

Normalising the simulated signal yields to data would require the knowledge of the abso-

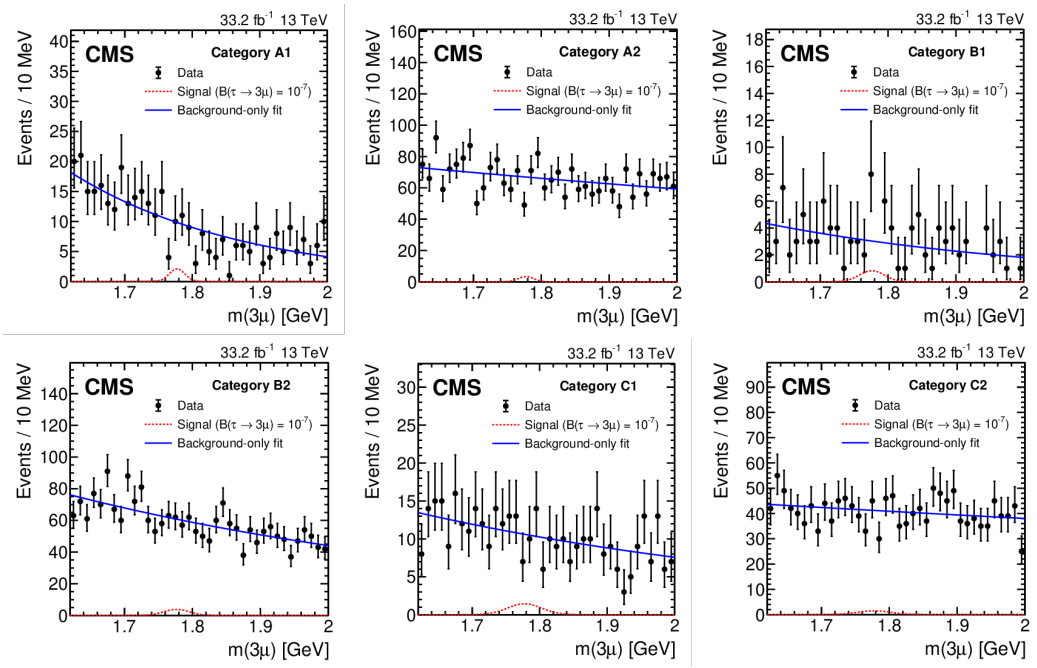

Figure 3: The $m(3\mu)$ invariant mass distributions in the six independent event categories used in the analysis in the HF channel. Data (black dots) are fitted to an exponential function in the background-only hypotesis (blue line), while the expected signal (red line) is estimated from simulation assuming $\mathcal{B}(\tau \to 3\mu) = 10^{-7}$ [6].

lute production cross section of D and B mesons. Moreover, it would involve a precise determination of the reconstruction and trigger efficiencies. The $D_s \to \phi(\mu\mu)\pi$ channel is therefore used to normalise the simulated signal yields to data with reduced systematic uncertainties.

The expected $\tau \to 3\mu$ signal yield can be expressed in terms of yield of D_s meson production, accounting for about 70% of the expected tau leptons produced in pp collisions, while the expected signal yield from B decays cannot be directly normalized by $D_s \to \phi(\mu\mu)\pi$. Nevertheless, the consistency between the $B^0, B^\pm$ and the D_s meson production rates can be tested by discriminating the prompt D_s and $B \to D_s$ contributions to the total D_s meson production. These two components can be discriminated in terms of decay length which can be used to measure the ratio between the prompt and $B \to D_s$ yields in data and MC.

Figure 4 shows the $\mu\mu\pi$ mass distribution fit with an exponential function for the background and two Crystal Ball functions for the $D^\pm$ and the $D_s^\pm$ peaks. From the fit, the number of produced D_s meson in data is extracted and compared to MC. The resulting scale factor is used to correct the simulated signal yields.

3 Analysis in the W channel

The second source of tau leptons at the LHC is the decay of W bosons. Despite the small contribution to the tau lepton production if compared to the D and B meson decays ($\sim 0.01\%$), $W \to \tau\nu$ decays provide a clean experimental signature, being characterised by lower background and higher trigger and selection efficiencies with respect to the HF channel, the tau leptons being produced at high momenta with a large missing energy due to the neutrino escaping detection, resulting in three muons produced in a narrow isolated cone.

Simulated Monte Carlo samples are used to model the signal and estimate the production of τ leptons, and to determine the acceptance and efficiency of the signal. The simulated

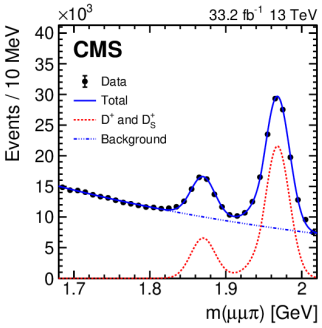

Figure 4: The $m(\mu\mu\pi)$ invariant mass distribution in data (black dots). The distribution is fit to an exponential function (blue dashed line) and two Crystal Ball functions (red dashed line). The solid line represents the combined model [6].

$W \to \tau(3\mu)\nu$ signal sample is normalised to the number of produced W bosons in data by means of existing measurements of the W boson production cross section at LHC [11,12]. The expected signal yield is corrected to account for the reconstruction and trigger efficiencies in data.

3.1 Event selection and categorisation

The $\tau \to 3\mu$ event selection is similar to the one used for the HF analysis (Sec. 2.1). Additional selections are applied to remove events with opposite-charged muon pairs having 2μ invariant mass compatible with the η, $\rho(770)$, $\omega(783)$, $\phi(1020)$, J/ψ, $\psi(2S)$, $\Upsilon(1S)$, $\Upsilon(2S)$, $\Upsilon(3S)$ and Z.

The pp interaction vertex is chosen as the one with the largest summed-p_T of the physics objects associated to it. The missing transverse momentum is computed from the reconstructed jets and tracks associated to the PV. The reconstructed missing transverse momentum ($\vec{p}_T^{\,\text{miss}}$) and the transverse momentum of the τ candidate allow to reconstruct the W boson p_T . Furthermore, by using the known mass of W boson, it is possible the determine the longitudinal momentum of the neutrino, which is given by two solutions.

Events are categorised based on the pseudorapidity of the τ candidate into barrel ($|\eta| < 1.6$) and endcap ($|\eta| \geq 1.6$).

3.2 Training of the Boosted Decision Tree

Similarly as done in the HF analysis, a BDT is trained to better separate signal from background, where the signal is made of $W \to \tau(3\mu)\nu$ simulated events and background is described by data events in the 3μ mass sidebands.

A set of 18 observables is used in the training: the $p_T^{3\mu}$ and η of the τ candidate, the χ^2 of the 3μ vertex fit, the pointing angle, the significance of the SV-PV distance, a measure of the muon reconstruction quality for each final-state muon, the difference in longitudinal IP with respect to the PV for each pair of muons, the isolation of the τ candidate, p_T^{miss}, the W boson p_T , the difference in the azimuthal angle between the $\vec{p}_T^{\,\text{miss}}$ and $\vec{p}_T^{\,3\mu}$, the transverse W mass and the two solutions of the longitudinal momentum of the neutrino.

The BDT score is used to reject background-like events, where a threshold is set based on the most stringent expected exclusion limits, independently in barrel and endcap. The 3μ mass distributions for events passing the BDT selection are shown in Figure 5. The signal is modelled with a Gaussian function with fixed mean and width, as determined from fitting the simulated signal in each event category.

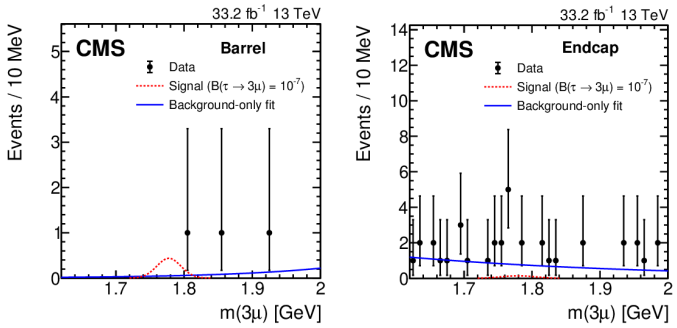

Figure 5: The $m(3\mu)$ invariant mass distributions in the two event categories used in the W channel analysis. Data (black dots) are fitted to an exponential function in the background-only hypotesis (blue line), while the expected signal (red line) is estimated from simulation assuming $\mathcal{B}(\tau \to 3\mu) = 10^{-7}$ [6].

4 Results

A simultaneous unbinned maximum likelihood fit to the $m(3\mu)$ distributions in the six categories of the HF analysis and the two categories of the W analysis is performed to extract the branching fraction $\mathcal{B}(\tau \to 3\mu)$. As shown in Figures 3 and 5, no evidence is found and upper limits on $\mathcal{B}(\tau \to 3\mu)$ are set using modified profile likelihood test statistics and the CLs criterion. Systematic uncertainties are incorporated in the analysis as nuisance parameters.

The largest systematic uncertainty for the HF channel is associated with the expected signal yield normalised to the $D_s \to \phi(\mu\mu)\pi$ channel, while in the W boson analysis the dominant source of uncertainty comes from the corrections used in extracting the signal trigger and reconstruction efficiences.

The observed (expected) upper limit at 90% CL on $\mathcal{B}(\tau \to 3\mu)$ is $8.0 \times 10^{-8} (6.9 \times 10^{-8})$.

5 Conclusion and perspectives

The search for $\tau \to 3\mu$ decays at the CMS experiment on data collected in 2016 has been presented. At the end of 2016, the CMS pixel detector underwent a significant upgrade which reflected in improved vertex and track reconstruction capabilities in 2017 and 2018 [13]. At the time of the conference, the analysis on the full Run 2 dataset, accounting for an integrated luminosity of $\sim$ 137 fb^{-1}, was at its final stage, being reviewed by the Collaboration. The higher statistics available for the Run 2 analysis will provide higher sensitivity to the search. Moreover, larger datasets will allow to better exploit multi-variate analysis techniques for the background rejection.

In Run 3, which will start in 2022, the CMS experiment is expected to collect an integrated luminosity of $\sim$ 200 fb^{-1}. A dedicated trigger for the $\tau \to 3\mu$ search is under development, aimed at lowering the muon p_T threshold to enhance the signal acceptance while keeping similar trigger rates as in 2018. Moreover, in Run 3 and beyond, new muon detectors based on the GEM technology [14] will improve the muon momentum resolution at trigger level and enlarge the pseudorapidity acceptance of the muon detector, thus increasing the acceptance of the CMS detector to the $\tau \to 3\mu$ signal.

References

[1] G. Hernández-Tomé, G. López Castro and P. Roig, *Flavor violating leptonic decays of τ and μ leptons in the Standard Model with massive neutrinos*, Eur. Phys. J. C **79**(1), 84 (2019), doi:10.1140/epjc/s10052-019-6563-4, [Erratum: Eur.Phys.J.C 80, 438 (2020)], 1807.06050.

[2] M. Giffels, J. Kallarackal, M. Krämer, B. O'Leary and A. Stahl, *Lepton-flavor-violating decay $\tau \to \mu\mu\overline{\mu}$ at the CERN LHC*, Phys. Rev. D **77**, 073010 (2008), doi:10.1103/PhysRevD.77.073010.

[3] K. S. Babu and C. Kolda, *Higgs-Mediated $\tau \to 3\mu$ in the Supersymmetric Seesaw Model*, Phys. Rev. Lett. **89**, 241802 (2002), doi:10.1103/PhysRevLett.89.241802.

[4] Belle Collaboration, *Search for lepton-flavor-violating τ decays into three leptons with 719 million produced $\tau^+\tau^-$ pairs*, Physics Letters B **687**(2-3), 139–143 (2010), doi:10.1016/j.physletb.2010.03.037.

[5] CMS Collaboration, *The CMS experiment at the CERN LHC*, Journal of Instrumentation **3**(08), S08004 (2008), doi:10.1088/1748-0221/3/08/s08004.

[6] CMS Collaboration, *Search for the lepton flavor violating decay $\tau \to 3\mu$ in proton-proton collisions at $\sqrt{s} = 13$ TeV*, Journal of High Energy Physics **2021**(1) (2021), doi:10.1007/jhep01(2021)163.

[7] BABAR Collaboration, *Limits on lepton-flavor violating decays into three charged leptons*, Physical Review D **81**(11) (2010), doi:10.1103/physrevd.81.111101.

[8] LHCb collaboration, *Search for the lepton flavour violating decay $\tau^- \to \mu^-\mu^+\mu^-$*, Journal of High Energy Physics **2015**(2), 121 (2015), doi:10.1007/JHEP02(2015)121.

[9] ATLAS Collaboration, *Probing lepton flavour violation via neutrinoless $\tau \to 3\mu$ decays with the ATLAS detector*, The European Physical Journal C **76**(5) (2016), doi:10.1140/epjc/s10052-016-4041-9.

[10] CMS Collaboration, *Search for $\tau \to 3\mu$ decays using τ leptons produced in D and B meson decays*, Tech. Rep. CMS-PAS-BPH-17-004, CERN, Geneva (2019).

[11] ATLAS Collaboration, *Measurement of $W^\pm$ and Z-boson production cross sections in pp collisions at $\sqrt{s} = 13$ TeV with the ATLAS detector*, Physics Letters B **759**, 601–621 (2016), doi:10.1016/j.physletb.2016.06.023.

[12] Particle Data Group, *Review of Particle Physics*, PTEP **2020**(8), 083C01 (2020), doi:10.1093/ptep/ptaa104.

[13] CMS Collaboration, *The CMS Phase-1 Pixel Detector Upgrade*, JINST **16**, P02027. 84 p (2020), doi:10.1088/1748-0221/16/02/P02027, 2012.14304.

[14] CMS Collaboration, *CMS Technical Design Report for the Muon Endcap GEM Upgrade*, Tech. Rep. CERN-LHCC-2015-012, CMS-TDR-013 (2015).